

# **Supporting Information for**

## **Zeolite-Encapsulated Ultrasmall Cu/ZnO<sub>x</sub> Nanoparticles for the Hydrogenation of CO<sub>2</sub> to Methanol**

Wen-Gang Cui,<sup>a</sup> Yan-Ting Li,<sup>a</sup> Lei Yu,<sup>a</sup> Hongbo Zhang,<sup>a</sup> Tong-Liang Hu<sup>a,b,c\*</sup>

<sup>[a]</sup> School of Materials Science and Engineering, Tianjin Key Laboratory of Metal and Molecule-Based Material Chemistry, National Institute for Advanced Materials, Nankai University, Tianjin 300350, China.

<sup>[b]</sup> State Key Laboratory of Coordination Chemistry, Nanjing University, Nanjing 210023, China.

<sup>[c]</sup> Tianjin Key Lab for Rare Earth Materials and Applications, Nankai University, Tianjin 300350, China.  
E-mail: tlhu@nankai.edu.cn (T.-L. Hu)

<b>Supporting Tables</b> .....	S-4
<b>Table S1.</b> The experimental details including the composition of the initial solutions, and amount of added monomer stock solution. ....	S-4
<b>Table S2.</b> Structural parameters of various catalysts. ....	S-5
<b>Supporting Figures</b> .....	S-6
<b>Figure S1.</b> Photograph of a typical reactor for the synthesis of nano-HKUST-1 in this work. ....	S-6
<b>Figure S2.</b> XRD patterns of Cu-HKUST-1, CuZn <sub>(1/2)</sub> -HKUST-1, CuZn <sub>(1/1)</sub> -HKUST-1, and CuZn <sub>(2/1)</sub> -HKUST-1 NPs.....	S-7
<b>Figure S3.</b> SEM images of (a) Cu-HKUST-1, (c) CuZn <sub>(1/2)</sub> -HKUST-1, (e) CuZn <sub>(1/1)</sub> -HKUST-1, and (g) CuZn <sub>(2/1)</sub> -HKUST-1 NPs. The corresponding size distribution histograms of (b) Cu-HKUST-1, (d) CuZn <sub>(1/2)</sub> -HKUST-1, (f) CuZn <sub>(1/1)</sub> -HKUST-1, and (h) CuZn <sub>(2/1)</sub> -HKUST-1 NPs obtained from SEM analysis. ....	S-8
<b>Figure S4.</b> XRD patterns of Na-ZSM-5, Cu/ZnO <sub>x</sub> /Na-ZSM-5, Cu@Na-ZSM-5, and Cu/ZnO <sub>x</sub> @Na-ZSM-5 samples with different mass ratios of Cu/Zn.....	S-9
<b>Figure S5.</b> SEM images of obtained ZSM-5 sample. ....	S-10
<b>Figure S6.</b> (a,b) SEM images of Cu@Na-ZSM-5 sample; (c,d) TEM images and corresponding element mapping images of Cu@Na-ZSM-5; (e) high-resolution TEM image of Cu@Na-ZSM-5 and (f) corresponding size distribution of Cu NPs.....	S-11
<b>Figure S7.</b> (a,b) SEM images of Cu/ZnO <sub>x</sub> (0.48)@Na-ZSM-5 sample; (c,d) TEM images and corresponding element mapping analyses images of Cu/ZnO <sub>x</sub> (0.48)@Na-ZSM-5; (e) high-resolution TEM image of Cu/ZnO <sub>x</sub> (0.48)@Na-ZSM-5 and (f) corresponding size distribution of Cu/ZnO <sub>x</sub> NPs. ....	S-12
<b>Figure S8.</b> (a,b) SEM images of Cu/ZnO <sub>x</sub> (2.23)@Na-ZSM-5 sample; (c,d) TEM images and corresponding element mapping analyses images of Cu/ZnO <sub>x</sub> (2.23)@Na-ZSM-5; (e) high-	

resolution TEM image of Cu/ZnO <sub>x</sub> (2.23)@Na-ZSM-5 and (f) corresponding size distribution of Cu/ZnO <sub>x</sub> NPs .....	S-13
<b>Figure S9.</b> TGA (black) and DTA (blue) of (a) raw-Cu@Na-ZSM-5, (b) raw-Cu/ZnO <sub>x</sub> (0.48)@Na-ZSM-5, (c) raw-Cu/ZnO <sub>x</sub> (1.38)@Na-ZSM-5, (d) raw-Cu/ZnO <sub>x</sub> (2.23)@Na-ZSM-5 measured from 30 to 800 °C in air at a heating rate of 10 °C·min <sup>-1</sup> . ....	S-14
<b>Figure S10.</b> (a) High-resolution TEM image of Cu/ZnO <sub>x</sub> /Na-ZSM-5 and (b) corresponding size distribution of Cu/ZnO <sub>x</sub> NPs.....	S-15
<b>Figure S11.</b> Dependences of the CO <sub>2</sub> conversion and product selectivity on temperature over Cu/ZnO <sub>x</sub> /Na-ZSM-5 catalyst.....	S-16
<b>Figure S13.</b> Dependences of the CO <sub>2</sub> conversion and product selectivity on temperature over Cu/ZnO <sub>x</sub> (2.23)@Na-ZSM-5 catalyst.....	S-18
<b>Figure S14.</b> Dependences of the CO <sub>2</sub> conversion and product selectivity on temperature over Cu/ZnO <sub>x</sub> (0.48)@Na-ZSM-5 catalyst.....	S-19
<b>Figure S15.</b> Dependences of the CO conversion and product selectivity on temperature over Cu/ZnO <sub>x</sub> (1.38)@Na-ZSM-5 catalyst.....	S-20
<b>Figure S16.</b> Data characterizing the influences of (a) velocity and (b) pressure to the performances of Cu/ZnO <sub>x</sub> (1.38)@Na-ZSM-5 catalyst in CO <sub>2</sub> hydrogenation.....	S-21
<b>Figure S17.</b> The durability of the industrial Cu/ZnO/Al <sub>2</sub> O <sub>3</sub> catalyst in CO <sub>2</sub> hydrogenation.....	S-22
<b>Figure S18.</b> In situ FTIR spectra of the CO <sub>2</sub> hydrogenation reaction on Cu@Na-ZSM-5 catalyst.....	S-23

## Supporting Tables

**Table S1.** The experimental details including the composition of the initial solutions, and amount of added monomer stock solution.

MOF	Concentration of added metal stock solution		AV <sup>b</sup> (mL)	CV <sup>c</sup> (mL)
	Metals <sup>a</sup>	Ligands		
Cu-HKUST-1	Cu(OAc) <sub>2</sub> ·H <sub>2</sub> O (Ethanol/DMF=1/1, 15 mM)	BTC (DMF, 10 mM)	40	40
CuZn <sub>(1/2)</sub> -HKUST-1	Cu(OAc) <sub>2</sub> ·H <sub>2</sub> O (Ethanol/DMF=1/1, 10 mM) Zn(OAc) <sub>2</sub> ·H <sub>2</sub> O (Ethanol/DMF=1/1, 20 mM)	BTC (DMF, 20 mM)	60	60
CuZn <sub>(1/1)</sub> -HKUST-1	Cu(OAc) <sub>2</sub> ·H <sub>2</sub> O (Ethanol/DMF=1/1, 15 mM) Zn(OAc) <sub>2</sub> ·H <sub>2</sub> O (Ethanol/DMF=1/1, 15 mM)	BTC (DMF, 20 mM)	60	60
CuZn <sub>(2/1)</sub> -HKUST-1	Cu(OAc) <sub>2</sub> ·H <sub>2</sub> O (Ethanol/DMF=1/1, 20 mM) Zn(OAc) <sub>2</sub> ·H <sub>2</sub> O (Ethanol/DMF=1/1, 10 mM)	BTC (DMF, 20 mM)	60	60

- a. Ethanol and DMF are added in form of volume ratio, respectively.
- b. Volume of added metal stock solution (mL).
- c. Volume of reaction solution collected after the reaction period (mL).

**Table S2.** Structural parameters of various catalysts.

Catalyst	Cu loading <sup>a</sup> (wt.%)	Zn loading <sup>a</sup> (wt.%)	Cu/Zn wt.%/ wt.%	S <sub>BET</sub> <sup>b</sup> (m <sup>2</sup> ·g <sup>-1</sup> )	S <sub>Micro</sub> <sup>b</sup> (m <sup>2</sup> ·g <sup>-1</sup> )	V <sub>Total</sub> <sup>b</sup> (cm <sup>3</sup> ·g <sup>-1</sup> ) <sup>c</sup>
ZSM-5	--	--	--	355	266	0.12
Cu/ZnO <sub>x</sub> /Na-ZSM-5	3.7	2.8	1.32	214	158	0.07
Cu@Na-ZSM-5	4.5	--	--	205	145	0.06
Cu/ZnO <sub>x</sub> (0.48)@Na-ZSM-5	2.2	4.6	0.48	198	166	0.08
Cu/ZnO <sub>x</sub> (1.38)@Na-ZSM-5	3.2	2.2	1.38	218	143	0.08
Cu/ZnO <sub>x</sub> (2.23)@Na-ZSM-5	4.8	2.15	2.23	223	160	0.05

a. Calculated from the results of ICP-OES.

b. S<sub>BET</sub> (total surface area), S<sub>Micro</sub> (micropore surface area), and V<sub>Total</sub> (total volume) were calculated using BET equation ( $0.05 < P/P_0 < 0.3$ ) of the adsorption isotherm.

## Supporting Figures

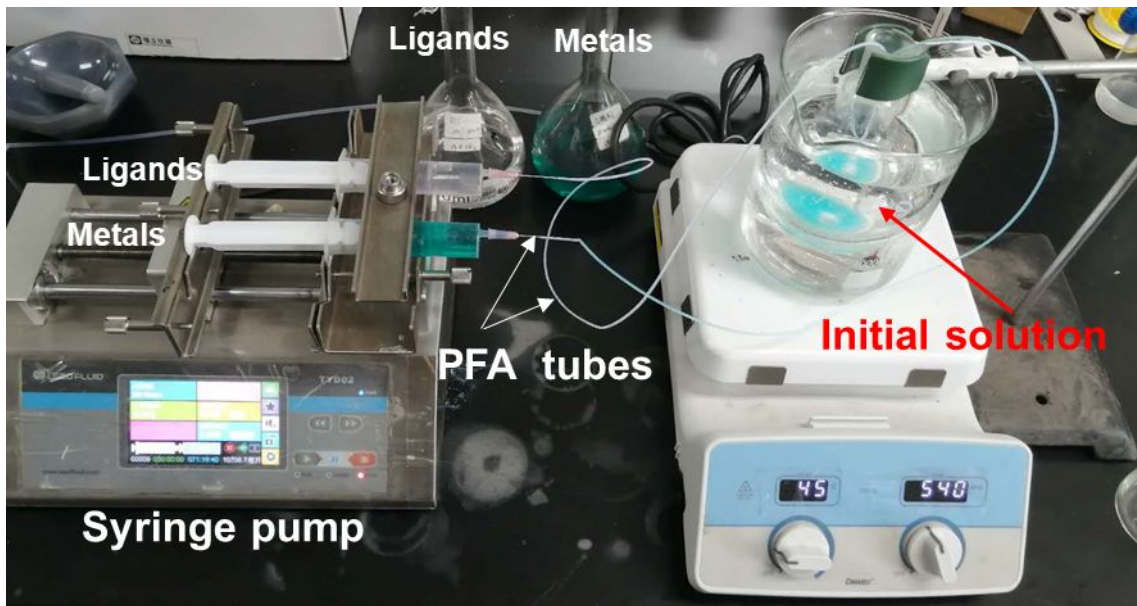


**Figure S1.** Photograph of a typical reactor for the synthesis of nano-HKUST-1 in this work.

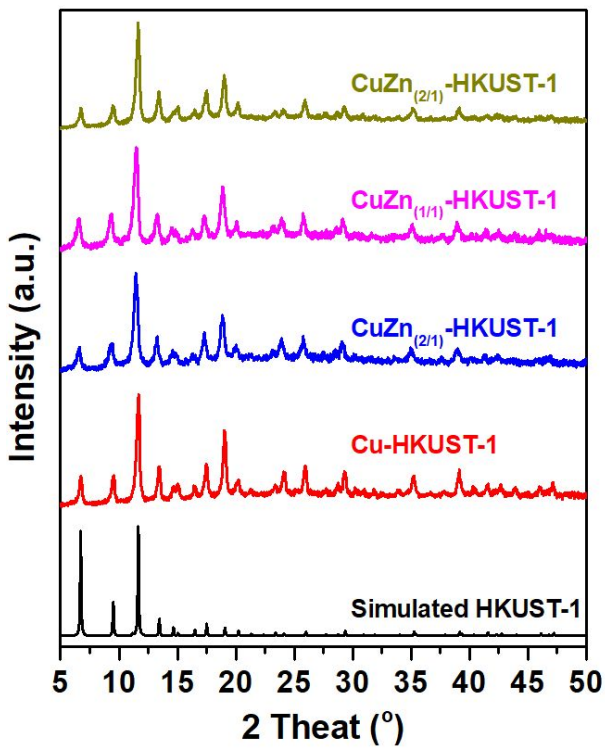


**Figure S2.** XRD patterns of Cu-HKUST-1,  $\text{CuZn}_{(1/2)}\text{-HKUST-1}$ ,  $\text{CuZn}_{(1/1)}\text{-HKUST-1}$ , and  $\text{CuZn}_{(2/1)}\text{-HKUST-1}$  NPs.

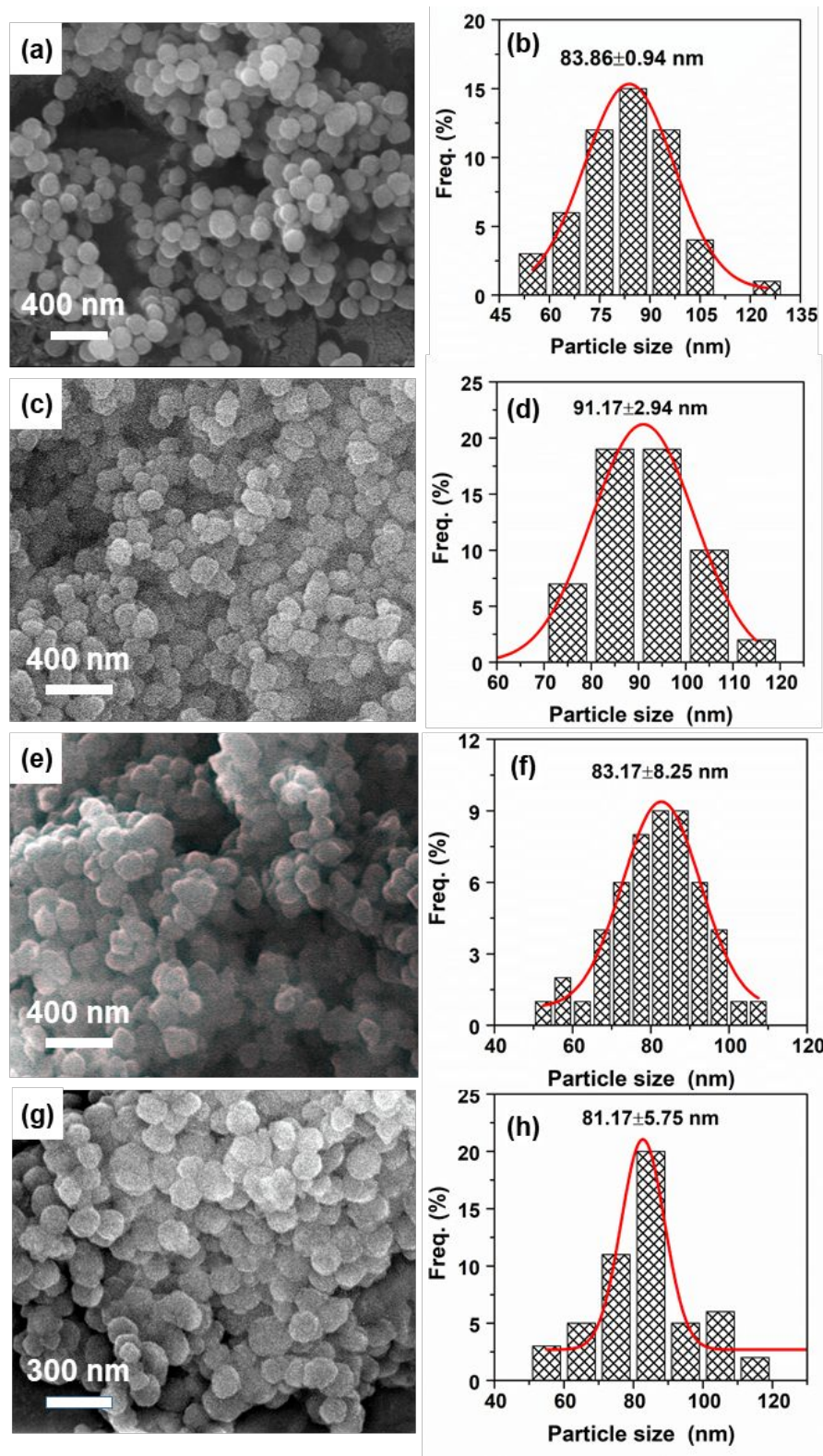


**Figure S3.** SEM images of (a) Cu-HKUST-1, (c) CuZn<sub>(1/2)</sub>-HKUST-1, (e) CuZn<sub>(1/1)</sub>-HKUST-1, and (g) CuZn<sub>(2/1)</sub>-HKUST-1 NPs. The corresponding size distribution histograms of (b) Cu-HKUST-1, (d) CuZn<sub>(1/2)</sub>-HKUST-1, (f) CuZn<sub>(1/1)</sub>-HKUST-1, and (h) CuZn<sub>(2/1)</sub>-HKUST-1 NPs obtained from SEM analysis.

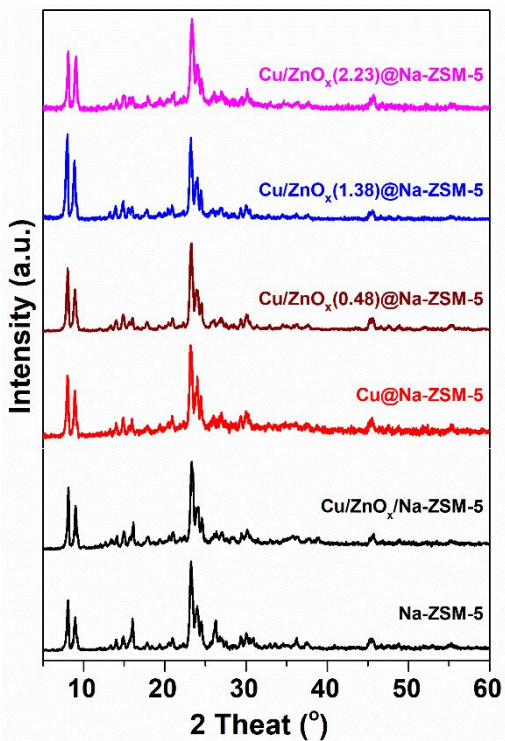


**Figure S4.** XRD patterns of Na-ZSM-5, Cu/ZnO<sub>x</sub>/Na-ZSM-5, Cu@Na-ZSM-5, and Cu/ZnO<sub>x</sub>@Na-ZSM-5 samples with different mass ratios of Cu/Zn. All samples exhibit XRD peaks associated with typical MFI zeolite structure. In addition, it is difficult to observe the peaks related to Cu or ZnO<sub>x</sub> crystals, indicating the high dispersion of the Cu/ZnO<sub>x</sub> species.

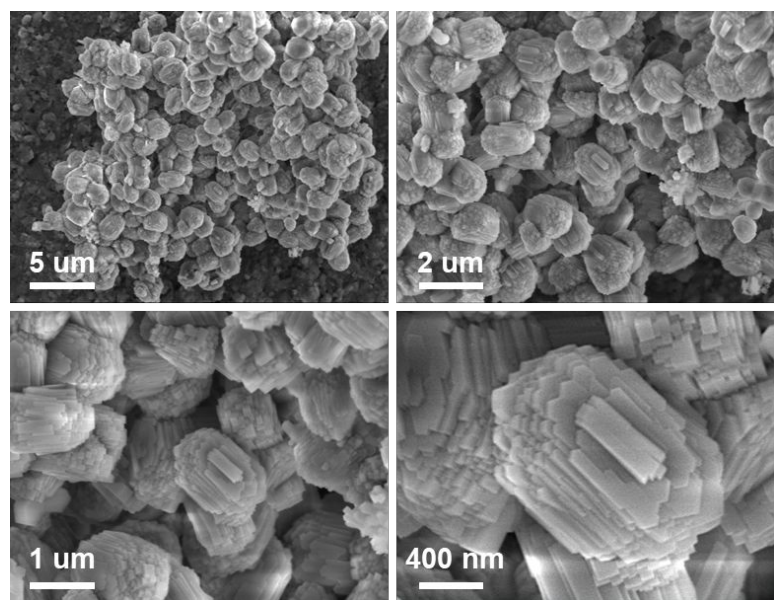


**Figure S5.** SEM images of obtained Na-ZSM-5 sample.

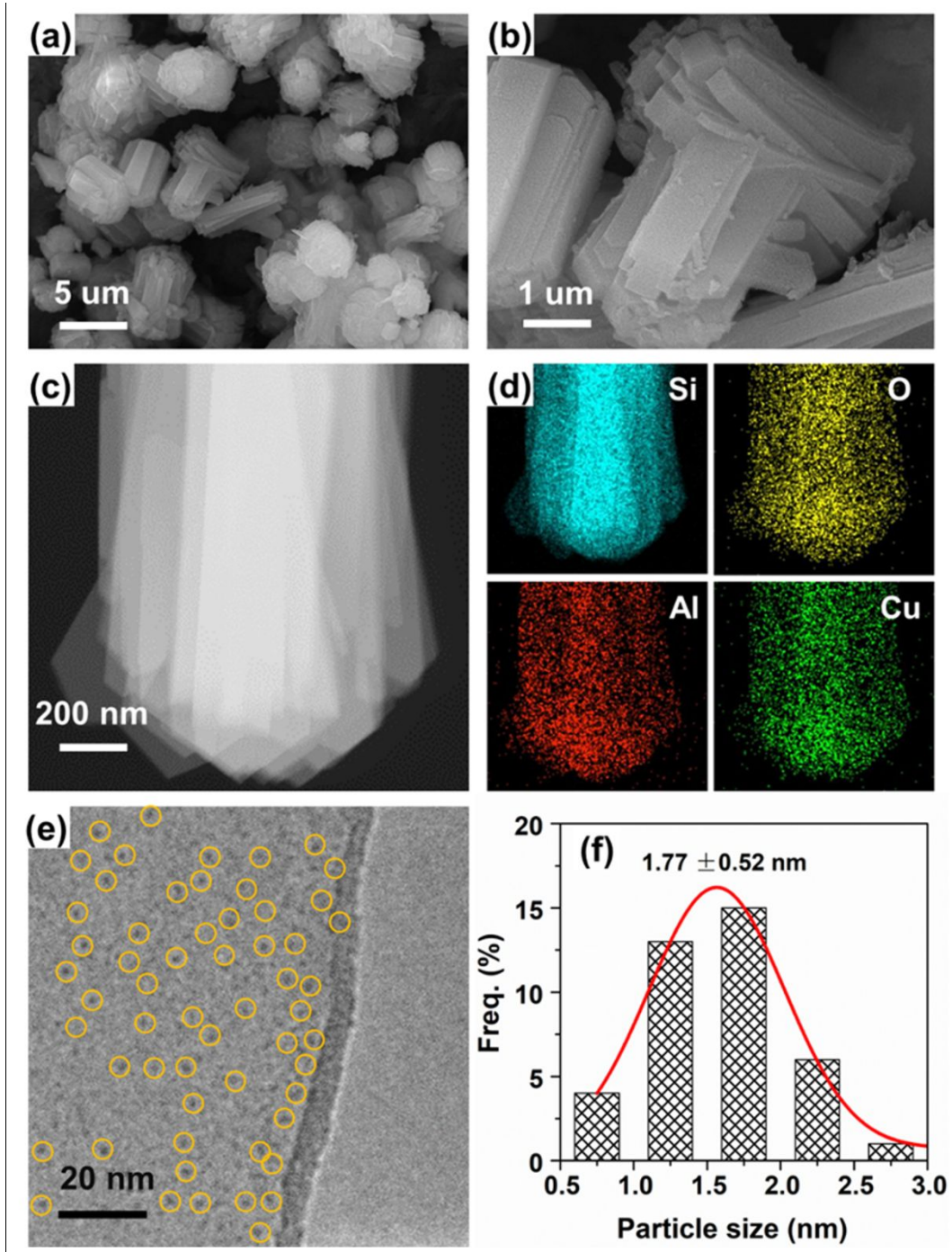


**Figure S6.** (a,b) SEM images of Cu@Na-ZSM-5 sample; (c,d) TEM images and corresponding element mapping images of Cu@Na-ZSM-5; (e) high-resolution TEM image of Cu@Na-ZSM-5 and (f) corresponding size distribution of Cu NPs.

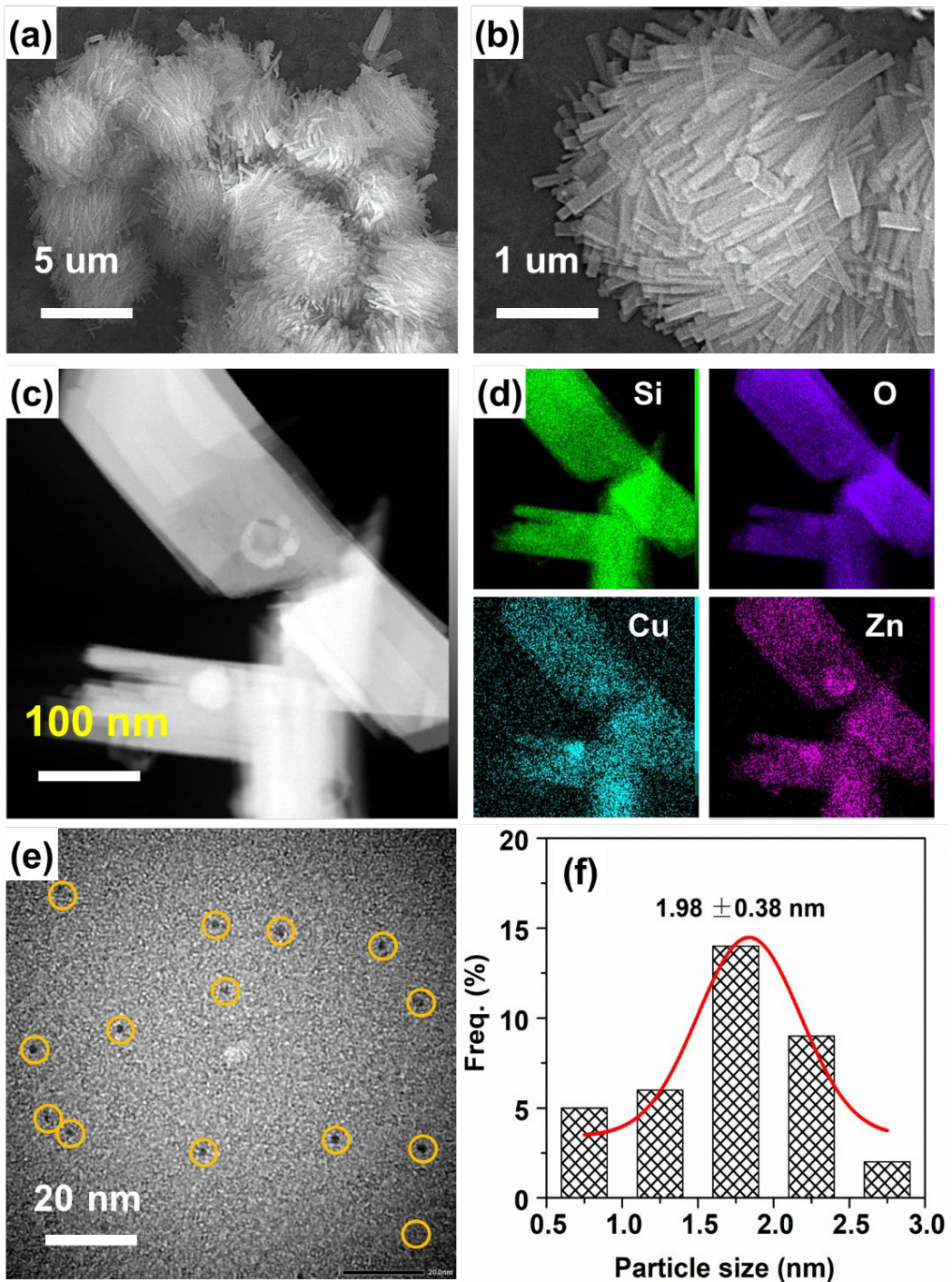


**Figure S7.** (a,b) SEM images of  $\text{Cu}/\text{ZnO}_x(0.48)\text{@Na-ZSM-5}$  sample; (c,d) TEM images and corresponding element mapping analyses images of  $\text{Cu}/\text{ZnO}_x(0.48)\text{@Na-ZSM-5}$ ; (e) high-resolution TEM image of  $\text{Cu}/\text{ZnO}_x(0.48)\text{@Na-ZSM-5}$  and (f) corresponding size distribution of  $\text{Cu}/\text{ZnO}_x$  NPs.

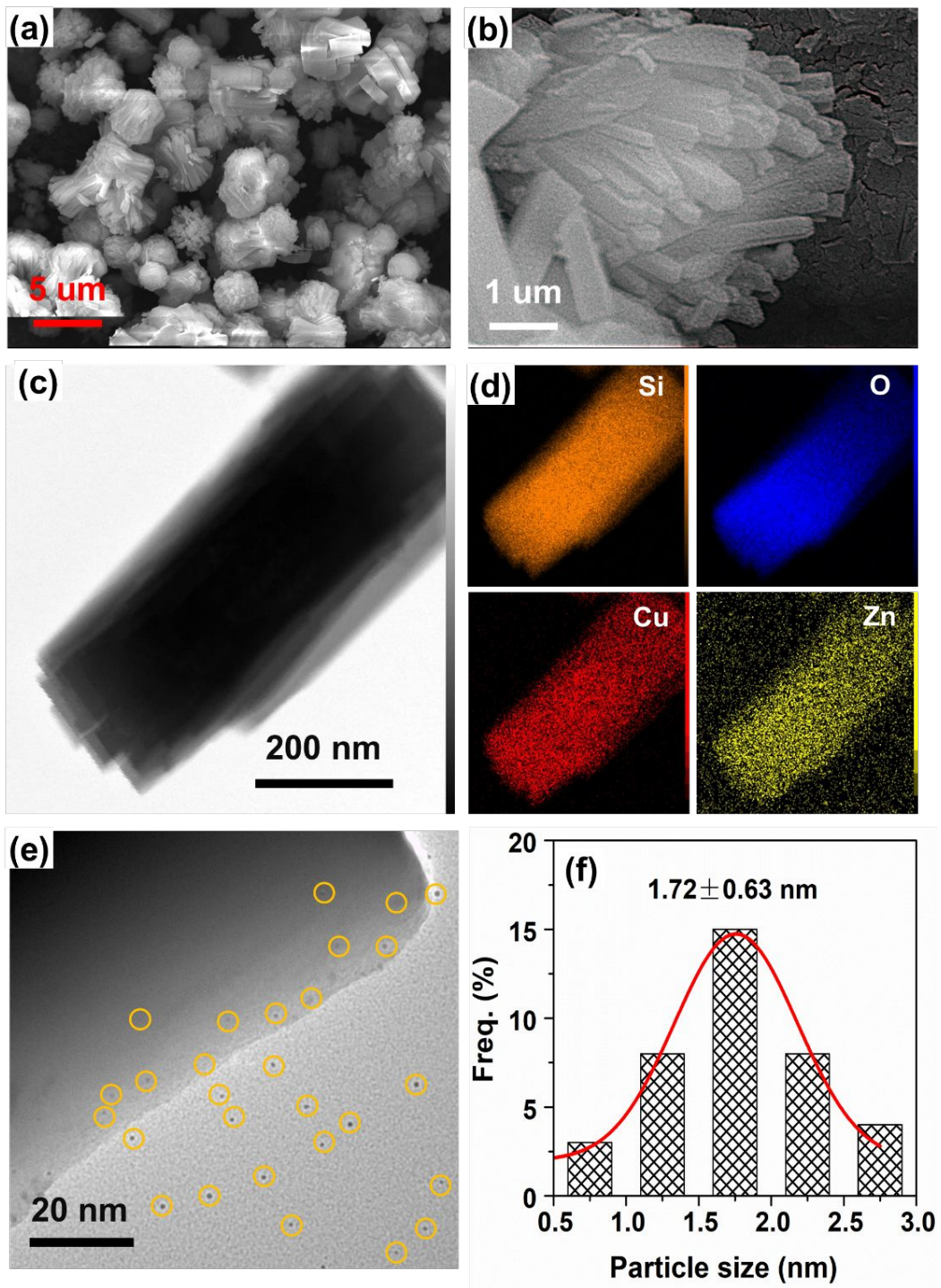


**Figure S8.** (a,b) SEM images of  $\text{Cu}/\text{ZnO}_x(2.23)\text{@Na-ZSM-5}$  sample; (c,d) TEM images and corresponding element mapping analyses images of  $\text{Cu}/\text{ZnO}_x(2.23)\text{@Na-ZSM-5}$ ; (e) high-resolution TEM image of  $\text{Cu}/\text{ZnO}_x(2.23)\text{@Na-ZSM-5}$  and (f) corresponding size distribution of  $\text{Cu}/\text{ZnO}_x$  NPs.

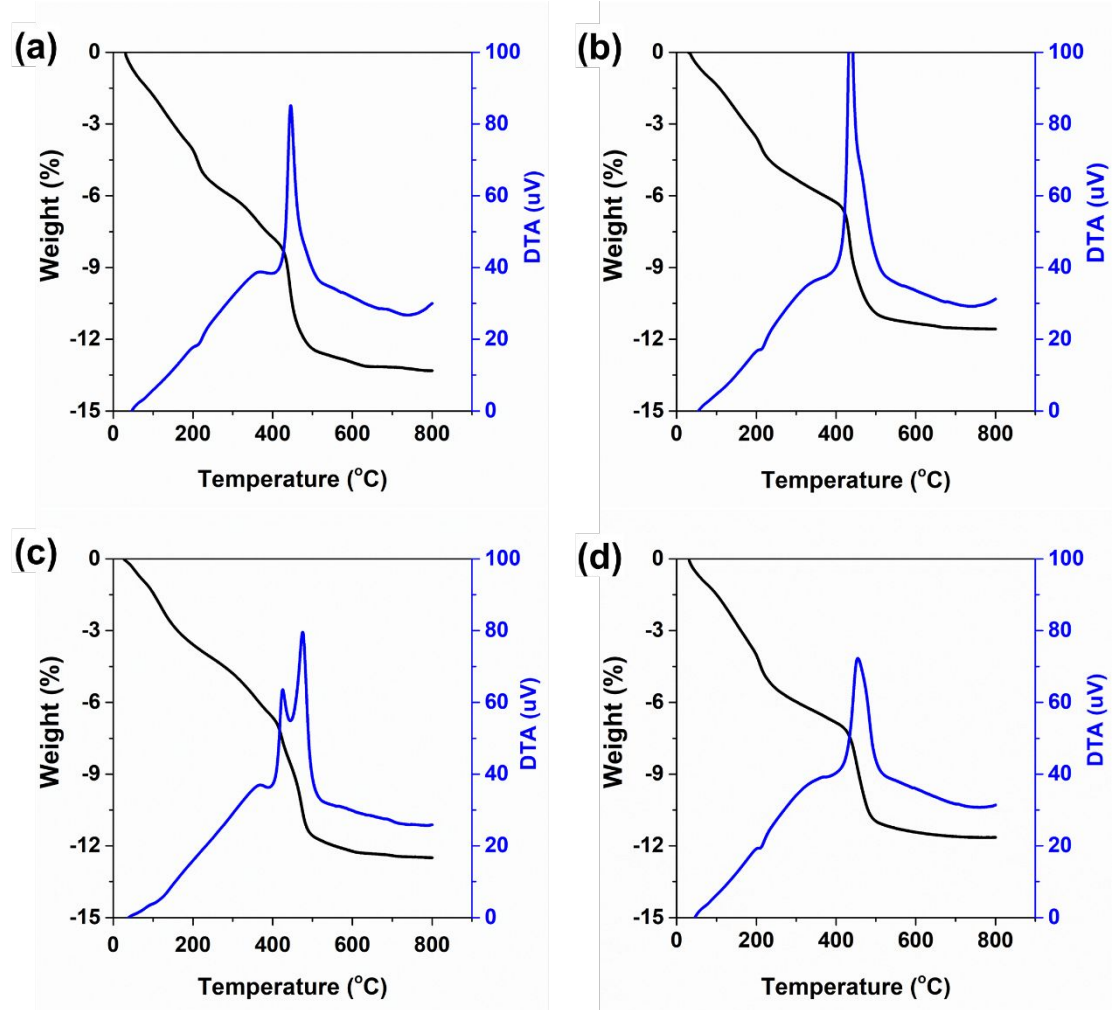


**Figure S9.** TGA (black) and DTA (blue) of (a) raw-Cu@Na-ZSM-5, (b) raw-Cu/ZnO<sub>x</sub>(0.48)@Na-ZSM-5, (c) raw-Cu/ZnO<sub>x</sub>(1.38)@Na-ZSM-5, (d) raw-Cu/ZnO<sub>x</sub>(2.23)@Na-ZSM-5 measured from 30 to 800 °C in air at a heating rate of 10 °C·min<sup>-1</sup>.

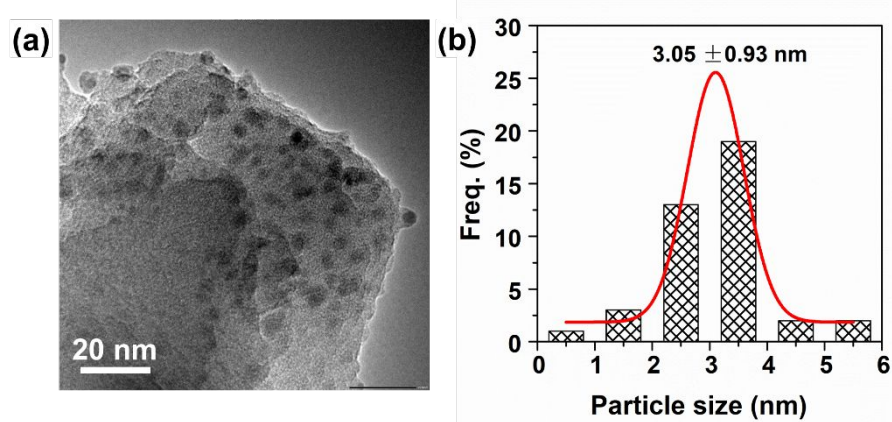


**Figure S10.** (a) High-resolution TEM image of Cu/ZnO<sub>x</sub>/Na-ZSM-5 and (b) corresponding size distribution of Cu/ZnO<sub>x</sub> NPs.

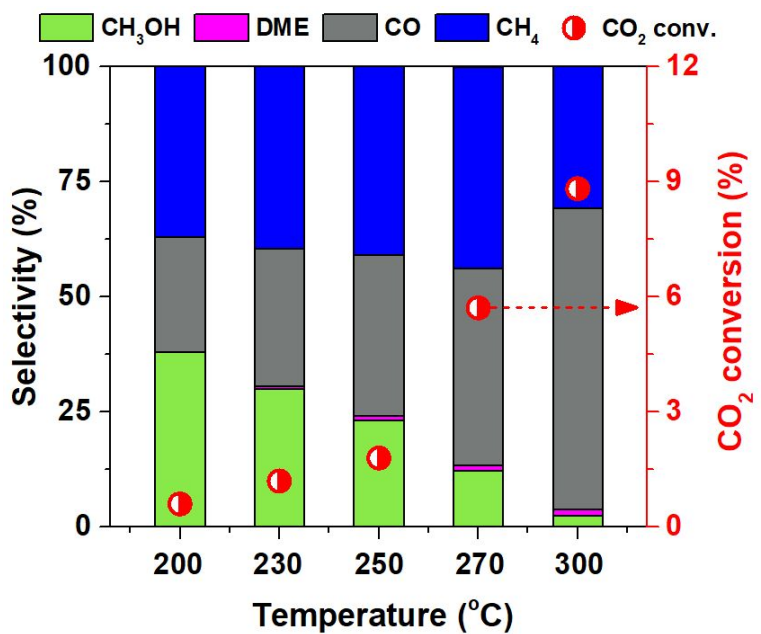


**Figure S11.** Dependences of the  $\text{CO}_2$  conversion and product selectivity on temperature over Cu/ZnO<sub>x</sub>/Na-ZSM-5 catalyst. Reaction conditions: 0.5 g of catalyst, 3.0 MPa,  $\text{H}_2/\text{CO}_2/\text{N}_2 = 71.5/23.5/5.0$ , and GHSV = 6,000  $\text{mL}\cdot\text{g}^{-1}\cdot\text{h}^{-1}$ .

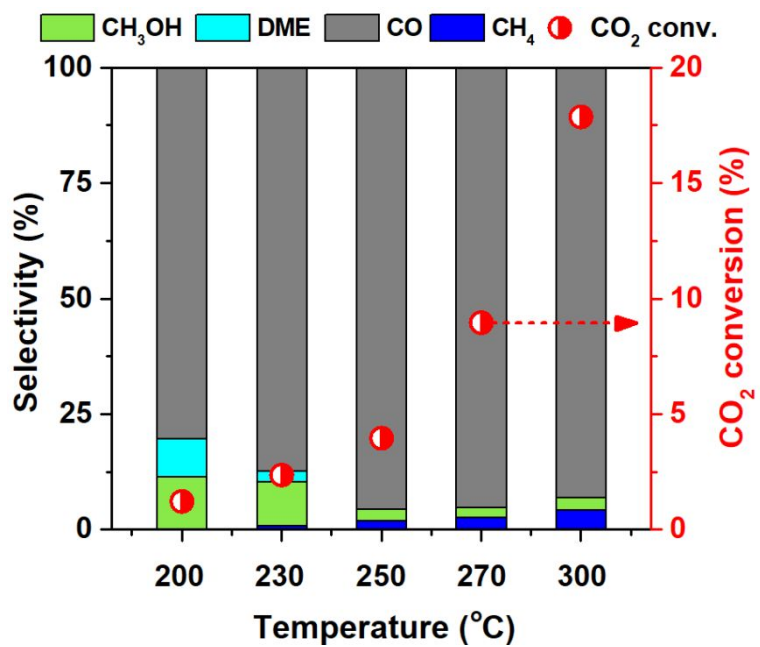


**Figure S12.** Dependences of the  $\text{CO}_2$  conversion and product selectivity on temperature over Cu@Na-ZSM-5 catalyst. Reaction conditions: 0.5 g of catalyst, 3.0 MPa,  $\text{H}_2/\text{CO}_2/\text{N}_2 = 71.5/23.5/5.0$ , and GHSV = 6,000  $\text{mL}\cdot\text{g}^{-1}\cdot\text{h}^{-1}$ .

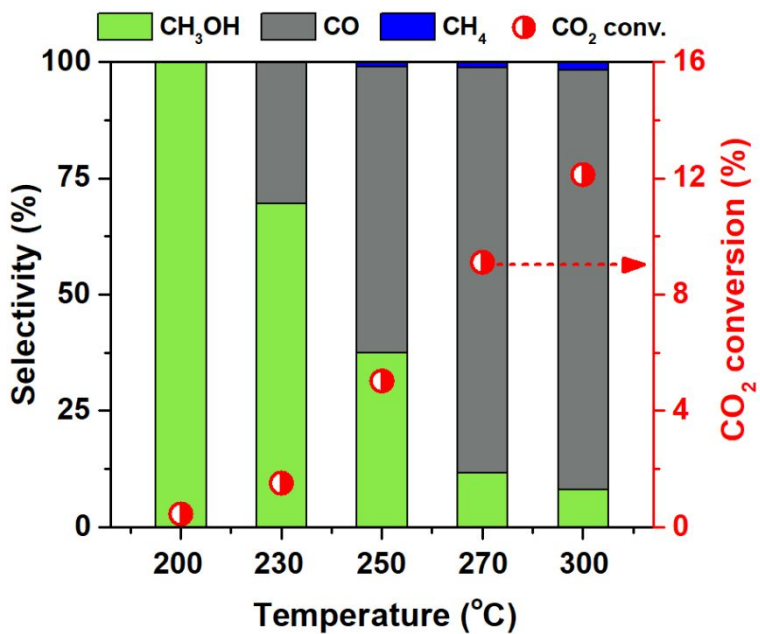


**Figure S13.** Dependences of the  $\text{CO}_2$  conversion and product selectivity on temperature over  $\text{Cu/ZnO}_x(2.23)@\text{Na-ZSM-5}$  catalyst. Reaction conditions: 0.5 g of catalyst, 3.0 MPa,  $\text{H}_2/\text{CO}_2/\text{N}_2 = 71.5/23.5/5.0$ , and GHSV = 6,000  $\text{mL}\cdot\text{g}^{-1}\cdot\text{h}^{-1}$ .

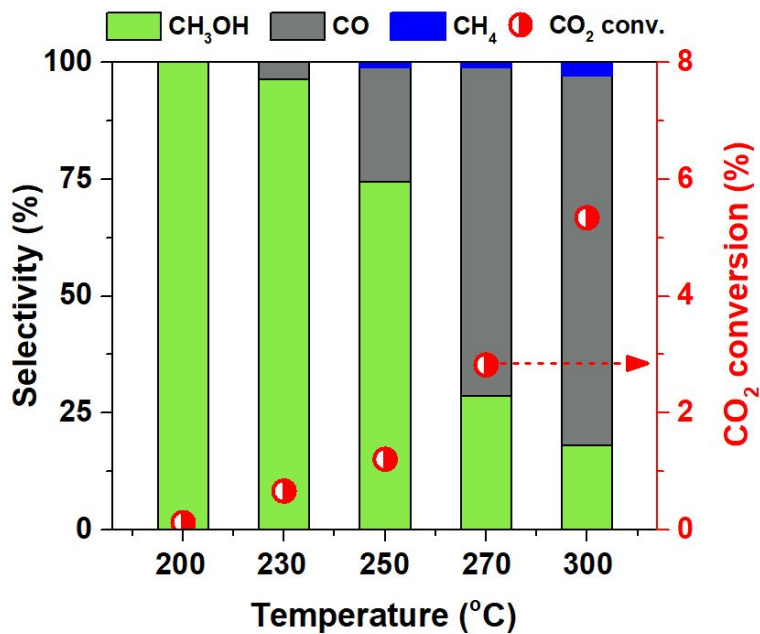


**Figure S14.** Dependences of the  $\text{CO}_2$  conversion and product selectivity on temperature over  $\text{Cu/ZnO}_x(0.48)@\text{Na-ZSM-5}$  catalyst. Reaction conditions: 0.5 g of catalyst, 3.0 MPa,  $\text{H}_2/\text{CO}_2/\text{N}_2 = 71.5/23.5/5.0$ , and GHSV = 6,000  $\text{mL}\cdot\text{g}^{-1}\cdot\text{h}^{-1}$ .

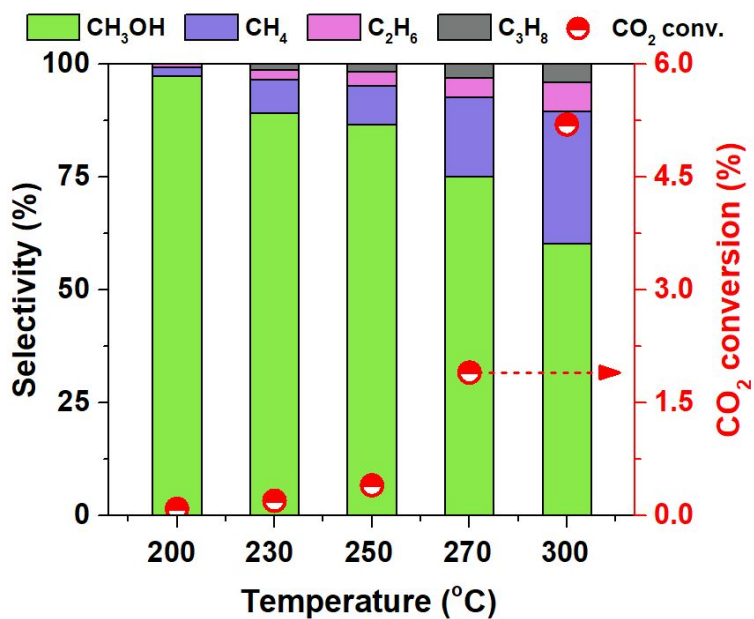


**Figure S15.** Dependences of the CO conversion and product selectivity on temperature over Cu/ZnO<sub>x</sub>(1.38)@Na-ZSM-5 catalyst. Reaction conditions: 0.5 g of catalyst, 3.0 MPa, H<sub>2</sub>/CO<sub>2</sub>/N<sub>2</sub> = 71.5/23.5/5.0, and GHSV = 6,000 mL·g<sup>-1</sup>·h<sup>-1</sup>.

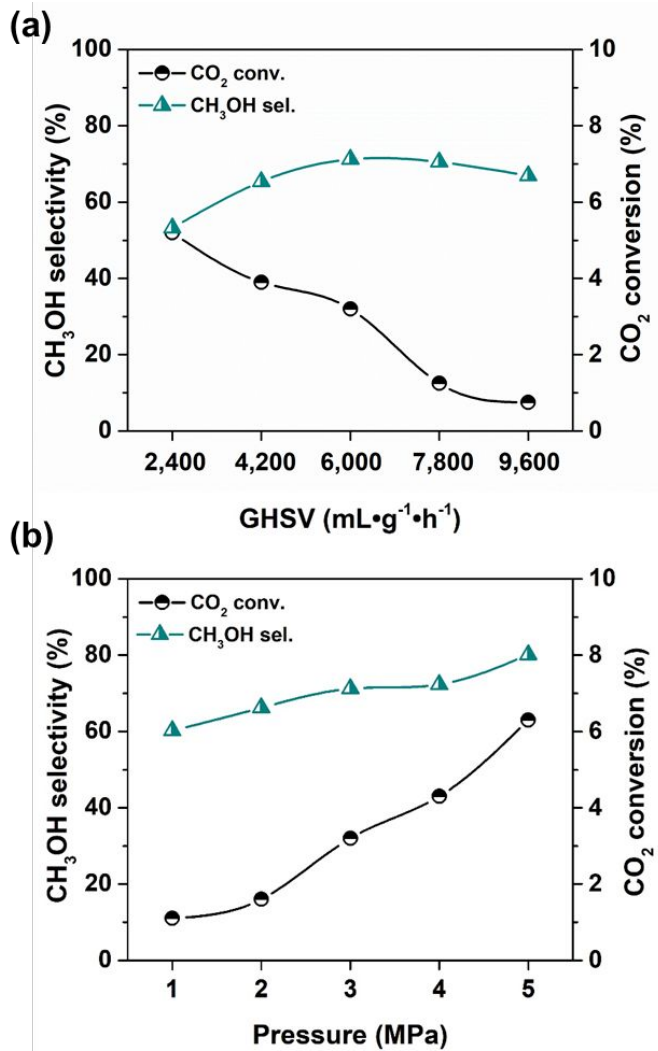


**Figure S16.** Data characterizing the influences of (a) velocity and (b) pressure to the performances of Cu/ZnO<sub>x</sub>(1.38)@Na-ZSM-5 catalyst in CO<sub>2</sub> hydrogenation. Standard reaction conditions: 0.5 g of Cu/ZnO<sub>x</sub>(1.38)@Na-ZSM-5 catalyst, 3.0 MPa, H<sub>2</sub>/CO<sub>2</sub>/N<sub>2</sub> = 71.5/23.5/5.0, 250 °C, and GHSV = 6,000  $\text{mL}\cdot\text{g}^{-1}\cdot\text{h}^{-1}$ .

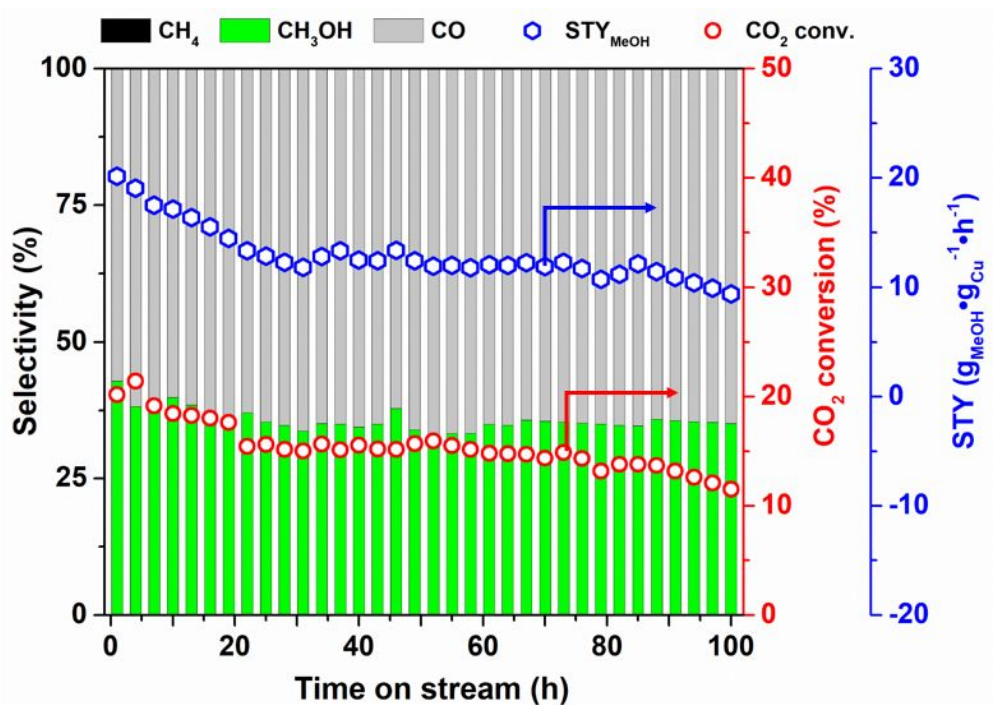


**Figure S17.** The durability of the industrial Cu/ZnO/Al<sub>2</sub>O<sub>3</sub> catalyst in CO<sub>2</sub> hydrogenation. Reaction conditions: GHSV = 6,000 mL·g<sub>cat</sub><sup>-1</sup>·h<sup>-1</sup>, 250 °C, 3.0 MPa, H<sub>2</sub>/CO<sub>2</sub>/N<sub>2</sub> = 71.5/23.5/5.0.

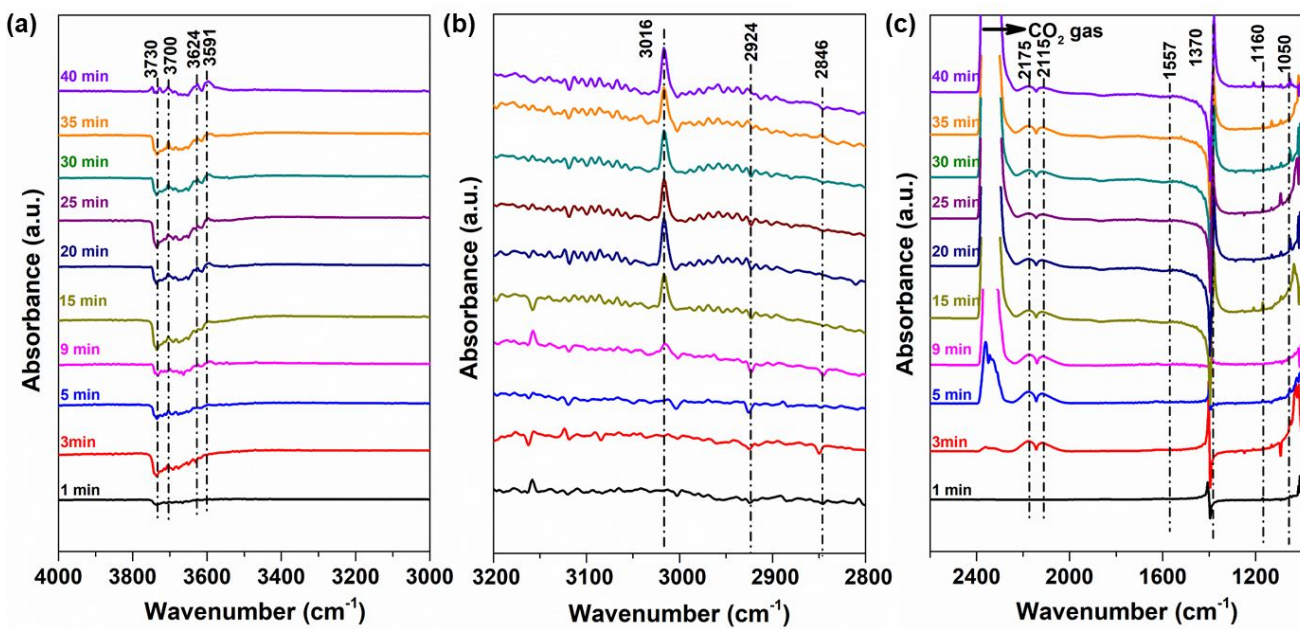


**Figure S18.** In situ FTIR spectra of the  $\text{CO}_2$  hydrogenation reaction on Cu@Na-ZSM-5 catalyst. The catalyst was exposed to 71.5% $\text{H}_2$ /23.5%  $\text{CO}_2$ /5% $\text{N}_2$  ( $20 \text{ mL}\cdot\text{min}^{-1}$ ) atmosphere at  $250^\circ\text{C}$  for 40 min.